The Dynamic Collapse of a Column Impacting a Rigid Surface

Jerrold M. Housner* and Norman F. Knight Jr.†
NASA Langley Research Center, Hampton, Virginia

An analytical investigation has been made of the dynamic collapse of an elastic periodically supported column having an attached mass at one end and impacting a rigid surface at the other end with prescribed velocity and angle of incidence. The investigation has been carried out using a first-order approximate nonlinear solution and a nonlinear finite element solution. The first-order approximate solution has led to the determination of four basic nondimensional parameters which govern the response. These parameters include mass, impact velocity, initial imperfection, and impact angle parameters. Three regions of these parameters have been identified in which the character of the column's response is markedly different. These regions have been designated as the linear, transition, and dynamic collapse regions. Threshold values of the parameters which separate these regions have been defined. Results obtained reveal that responses in the linear region are dominated by axial motion, those in the transition region exhibit some axial-flexural coupling, and those in the collapse region are dominated by flexure. The rebound velocity in the transition and dynamic collapse regions is shown to be less than that predicted by the linear dynamic solution. The dynamic peak axial compressive load in the transition region is shown to be the same as that predicted by the linear dynamic solution. In the collapse region, the peak load decreases to a value less than the linear dynamic value, but greater than the static Euler buckling load. Moreover, it is shown that whereas the peak axial compressive load predicted by the linear solution grows unbounded with increasing values of the mass parameter, an ultimate dynamic load value is approached in the collapse region.

Nomenclature

A = column cross-sectional area
C_R = coefficient of restitution, see Eq. (36)
$\tilde{C}$ = damping matrix, see Eq. (29)
c = speed of sound in column material, $\sqrt{E/\rho}$
E = elastic modulus
e = amplitude of initial imperfection, see Eq. (3)
$\tilde{e}$ = e/r
F = force vector of Eq. (30)
f = amplitude of column flexural motion, see Eq. (2)
$\tilde{f}$ = f/r
I = column moment of inertia
ℓ = length of column
M = column bending moment
$\tilde{M}$ = mass matrix defined in Eq. (30)
m_a = attached mass
m_c = column mass, $\rho A\ell$
$\tilde{m}$ = nondimensional mass parameter, see Eqs. (27)
N = number of periodic bays
P = column axial load
$\tilde{P}$ = ratio of P_{avg} to P_E
P_E = Euler buckling load, $EA\epsilon_E$
P_{avg} = average axial load
$\tilde{P}_1$ = ratio of P at $x=0$ to P_E
q = displacement vector defined in Eq. (30)
r = cross-sectional radius of gyration, $\sqrt{I/A}$
t = time
T = kinetic energy
U = column strain energy
$u,\hat{u}$ = axial displacements parallel to x and $\hat{x}$ axes, respectively
$\tilde{u}$ = nondimensional displacement parallel to x axis as defined in Eq. (20)
$\tilde{u}_R$ = nondimensional rebound displacement
v_0 = initial velocity of mass and column in negative x direction
$\tilde{v}$ = nondimensional impact velocity parameter defined in Eqs. (27)
$w,\hat{w}$ = flexural displacements of column in global and local coordinates, respectively
$\hat{w}_c,\hat{w}_d$ = convection and deformation components of $\hat{w}$, respectively
x,y = global column coordinates, see Fig. 1
$\hat{x},\hat{y}$ = local column coordinates, see Fig. 1
α = impact angle of column measured counterclockwise from surface normal, see Fig. 1
$\tilde{\alpha}$ = nondimensional impact angle parameter defined in Eqs. (27)
ϵ_m = axial strain at neutral axis of the column
ϵ_E = Euler buckling strain, see Eq. (21)
ρ = mass density of column material
τ = nondimensional time parameter

Subscripts

0 = evaluated at $x=\ell$
1 = evaluated at $x=0$

Introduction

THE ability to predict analytically the response of structural components to impact loading conditions plays an important role in the design of advanced structural systems. For example, research has recently focused on enhanced occupant survivability under specified aircraft crash conditions.[1] Finite element computer codes of various levels of sophistication have been developed[2-6] and are being applied to study and to predict aircraft response in crash environments.[3,6-10] In addition, full-scale crash tests on general aviation aircraft are being performed.[10-12] Likewise, large space structures composed of lightweight, flexible, structural elements may experience transient impact conditions from docking maneuvers and from foreign objects.

Impact responses can be quite complex, involving short-time transient and high-frequency components. Moreover,

Presented as Paper 82-0735 at the AIAA/ASME/ASCE/AHS 23rd Structures, Structural Dynamics and Materials Conference, New Orleans, La., May 10-12, 1982; submitted May 12, 1982; revision received Nov. 3, 1982. This paper is declared a work of the U.S. Government and therefore is in the public domain.

*Aerospace Engineer, Structural Dynamics Branch, Structures and Dynamics Division.
†Aerospace Engineer, Structural Mechanics Branch, Structures and Dynamics Division.

impact responses are often nonlinear. Reducing test data and analytical results to meaningful quantities for design, defining an adequate finite element model and assessing the accuracy of computer-generated results for such problems can be both difficult and tedious tasks. However, the understanding of similar, but simpler, structures as subelements of the more complex structure can guide the use of sophisticated computerized structural analyses when applied to the more complex structure. In addition, studies based on the simpler structure can aid in the interpretation of measured and calculated results and lead to the development of scaling laws for model testing.

A fundamental structural problem having a bearing on the impact response of structural components is the dynamic collapse of a column under axial impact. The problem of a periodically supported column with an attached mass at one end and impacting a rigid surface with prescribed velocity and angle of incidence at the other end contains features common to both aircraft and large space structural components. For example, in an aircraft, the column may represent a longeron, the periodic supports may represent the column collapse restraining mechanism introduced by periodic frames or rings in the fuselage, and the attached mass may represent the mass of the aircraft aft of the section which suffers the impact. In a periodic space truss, the column may represent a truss member which is to be docked to another structure, the periodic supports may represent the collapse restraint offered by other members of the truss which attach to the column at periodic joints along its length, and the attached mass may represent the mass of the truss aft of the section which suffers the impact.

There is a considerable amount of literature on the dynamic collapse of columns.[13-22] Such work generally falls into the following three categories: 1) prescribed time-varying axial forces at the ends of the column, 2) prescribed constant axial velocity at one end of the column with the other end restrained, and 3) prescribed initial axial velocity of an impacting mass at one end of the column with the other end restrained. Although none of the references treated periodic columns with an attached mass, an angle of incidence, or contact conditions, many of their conclusions are still applicable inasmuch as all three categories, especially the second and third, have much in common with the present problem.

Hoff[13,14] investigated the effect of a moving head of a testing machine on the measured collapse of simply supported columns and his work is representative of a column in the second category. This problem is also representative of a column in the third category when the ratio of the attached mass to column mass becomes very large. Hoff made certain assumptions on the deformation behavior, neglected axial inertia and thus axial wave motion, and assumed an initial half sine wave deformation shape whose magnitude grows during collapse, but whose shape remains fixed. References 15, 19, and 20 indicate that these assumptions are valid for columns in the third category except at very high impact velocities. Hoff established a nondimensional dynamic similarity parameter which permits a scientific definition of "high velocity" for this case. This parameter involves the speed of sound in the column material, the Euler buckling strain of the column, and the initial impact velocity which in Hoff's problem is the column end velocity at all times. Using the results of Refs. 15, 19, and 20 and interpreting the results therein in terms of Hoff's similarity parameter, one concludes that Hoff's deformation assumptions should be reasonably valid for many applications. For example, his assumptions are valid for studying the crash behavior of aircraft with conventional aluminum construction, with member buckling strains greater than 0.001 and impact velocities less than 26 m/s (60 mph) or the impact response of space trusses with a graphite-epoxy construction, member slenderness ratios less than 500, and impact velocities less than 0.88 m/s (2 mph). It is therefore reasonable to extend his formulation to establish a first-order approximate nonlinear solution to the present problem.

The purpose of this paper is to present the results of an analytical investigation on the dynamic collapse of an elastic periodically supported column. The column has an attached mass at one end and impacts a rigid surface with prescribed velocity and angle of incidence at the other end. Column to rigid-surface contact and rebound are accounted for in the analysis.

A first-order approximate nonlinear analysis is developed in which it is assumed that axial wave motion is negligible, that the deformation shape of the column is a half sine wave in each periodic bay, and that only first-order nonlinear terms need be retained. The differential equations of the problem are derived in a manner which permits the governing basic nondimensional parameters to be easily assembled. The equations are then solved numerically by explicit time integration in order to determine specific ranges of these parameters for which the response characteristics are markedly different. To assess modeling sophistication relative to prediction accuracy, a comparison is made of the results from this approximate analysis with those of a finite element computer code based on a convected coordinate formulation. This code, developed using an approach similar to Refs. 23 and 24, does not place any restriction on the deformation shape of the column nor on its magnitude, thereby eliminating the restriction of moderate rotations inherent in all the previous column references.

Analysis

First-Order Approximate Nonlinear Solution

Assumed Displacement Shapes

Consider an elastic periodically supported column with an attached mass impacting a rigid surface at an angle α from the surface normal as shown in Fig. 1. Recognizing that a first-order approximate nonlinear theory is desired, the axial deformation for an Euler column is assumed to have the following form,

$$\hat{u}=\hat{u}_1+(\hat{x}/\ell)(\hat{u}_0-\hat{u}_1)-\hat{y}(\hat{w}_{,\hat{x}}-\hat{e}_{,\hat{x}}) \tag{1}$$

where a linear axial displacement is assumed and $\hat{u}$ and $\hat{w}$ are the local column axial and transverse displacements, respectively, $\hat{x}$ and $\hat{y}$ the local column coordinates, ℓ the column length, and $\hat{e}$ an initial column imperfection. The transverse displacement is assumed to be composed of a convection and a deformation part as,

$$\hat{w}=\hat{w}_c+\hat{w}_d$$

where

$$\hat{w}_c=\hat{w}_1+(\hat{x}/\ell)(\hat{w}_0-\hat{w}_1)$$

and

$$\hat{w}_d=f\sin(N\pi\hat{x}/\ell) \tag{2}$$

Also,

$$\hat{e}=e\sin(N\pi\hat{x}/\ell) \tag{3}$$

Thus, a sinusoidal shape has been assumed for the transverse deformation and the initial imperfection as in Refs. 13 and 14, and N is the number of periodic bays.

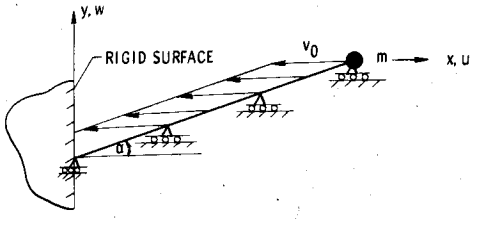

Fig. 1 Geometry and coordinate systems of an elastic periodically supported column impacting a rigid surface.

The displacements in the local column coordinates $(\hat{x}, \hat{y})$ are related to those in the global coordinates (x, y) by

$$\hat{u} = [u_1 + (\hat{x}/\ell)\, u_0 - u_1)]\cos\alpha - \hat{y}(N\pi/\ell)\,(f-e)\cos(N\pi\hat{x}/\ell) \tag{4}$$

$$\hat{w} = -[u_1 + (\hat{x}/\ell)\,(u_0 - u_1)]\sin\alpha + f\sin(N\pi\hat{x}/\ell) \tag{5}$$

since due to the periodic supports

$$w_1 = w(\ell/j) = 0; \quad j = 1,2,\ldots,N \tag{6}$$

Equations of Motion, Contact, and Initial Conditions

The equations of motion, contact, and initial conditions may be derived from Hamilton's principle

$$\int_0^{t^*} (\delta U - \delta T)\,\mathrm{d}t + \left[(m_c/\ell)\, v_0 \sin\alpha \int_0^{\ell} \delta\hat{w}\,\mathrm{d}\hat{x} - m_a v_0 \delta u_0\right]_0^{t^*} = 0 \tag{7}$$

where δU and δT are the variations of the strain and kinetic energies, respectively, m_a and m_c denote the attached mass and column mass, respectively, and v_0 the initial velocity of the mass and column in the negative x direction. Assuming a prismatic column

$$\delta U = \int_0^{\ell} (P_{\text{avg}}\delta\epsilon_m - M\delta w_{,\hat{x}\hat{x}})\,\mathrm{d}\hat{x} \tag{8}$$

where P_{avg} is the average axial column load, M the local column moment, ϵ_m the strain at the neutral axis which to first-order nonlinear terms is

$$\epsilon_m = (u_0 - u_1)\,(\cos\alpha)/\ell + \tfrac{1}{2}\left((\hat{w}_{d,\hat{x}})^2 - (\hat{e}_{,x})^2\right) \tag{9}$$

and it is recognized that the convected transverse motion does not give rise to strain. Substitution of Eqs. (2), (3), and (5) into Eq. (9) yields

$$\epsilon_m = (u_0 - u_1)\,(\cos\alpha)/\ell + \tfrac{1}{2}(N\pi/\ell)^2\,(f^2 - e^2)\cos^2(N\pi\hat{x}/\ell) \tag{10}$$

Using Eq. (10), the average axial column load P_{avg} is

$$P_{\text{avg}} = (EA/\ell)[(u_0 - u_1)\cos\alpha + \tfrac{1}{4}(N^2\pi^2/\ell)\,(f^2 - e^2)] \tag{11}$$

The column bending moment M is given by

$$M = EA\,(r/\ell)^2\,(N\pi)^2\,(f-e)\sin(N\pi\hat{x}/\ell) \tag{12}$$

where r is the cross-sectional radius of gyration. Substitution of Eqs. (11) and (12) and the variations of Eqs. (5) and (10) into Eq. (8) yields

$$\delta U = P_{\text{avg}}\cos\alpha\,(\delta u_0 - \delta u_1) + (N\pi)^2/(2\ell)[P_{\text{avg}} f + EA\,(r/\ell)^2\,(N\pi)^2\,(f-e)]\delta f \tag{13}$$

Using Eq. (5) and neglecting the axial inertia of the column gives

$$\begin{aligned}\delta T = m_c\{&[(\dot{u}_1/3 + \dot{u}_0/6)\sin^2\alpha - \dot{f}(\sin\alpha)/(N\pi)]\delta\dot{u}_1 \\ &+ [(\dot{u}_0/3 + \dot{u}_1/6)\sin^2\alpha + (-1)^N\dot{f}(\sin\alpha)/(N\pi)]\delta\dot{u}_0 \\ &+ [-\dot{u}_1(\sin\alpha)/(N\pi) + (-1)^N\dot{u}_0(\sin\alpha)/(N\pi) \\ &+ \tfrac{1}{2}\dot{f}]\delta\dot{f}\} + m_a\dot{u}_0\delta\dot{u}_0\end{aligned} \tag{14}$$

where $(\dot{})$ indicates differentiation with respect to time t. Finally, substituting Eqs. (13) and (14) into Eq. (7), integrating by parts and noting that the resulting equation must be valid for all variations yields three equations. Two of these equations are recognized as the equations of motion derived from the variations of u_0 and f; while the third equation is recognized as the column to rigid-surface contact condition derived from the variation of u_1. The resulting equations of motion are as follows:

$$\begin{aligned}&P_{\text{avg}}\cos\alpha + m_c[(\ddot{u}_0/3 + \ddot{u}_1/6)\sin^2\alpha \\ &\quad + (-1)^N\ddot{f}(\sin\alpha)/(N\pi)] + m_a\ddot{u}_0 = 0\end{aligned} \tag{15}$$

and

$$\begin{aligned}&(N\pi)^2/(2\ell)[P_{\text{avg}} f + (N\pi)^2\,(EA)\,(r/\ell)^2\,(f-e)] \\ &+ m_c[-\ddot{u}_1(\sin\alpha)/(N\pi) + (-1)^N\ddot{u}_0(\sin\alpha)/(N\pi) + \tfrac{1}{2}\ddot{f}] = 0\end{aligned} \tag{16}$$

The value of u_1 and its second derivative in Eqs. (15) and (16) are provided by the contact condition. It is assumed that the column and the rigid surface are in contact, provided the generalized force associated with the u_1 degree of freedom tends to put compression in the column. Thus,

$$u_1 = \begin{cases} 0, & \text{if } P_{\text{avg}} < 0 \\ u_R, & \text{if } P_{\text{avg}} = 0 \end{cases} \tag{17}$$

where u_R is given by the vanishing of Eq. (11), namely

$$u_R = u_0 + (N\pi)^2\,(f^2 - e^2)/(4\ell\cos\alpha) \tag{18}$$

and since the column cannot pass through the rigid surface, $u_R \geq 0$. The equations of motion are subject to the following initial conditions at $t = 0$ which may also be derived from Hamilton's principle,

$$\begin{aligned}&u_0 = u_1 = \dot{u}_1 = 0, \text{ and } f = e \\ &\dot{f} = 2v_0\{1 + (m_c/m_a)\,(\sin^3\alpha)/(N\pi)[1/3 + (-1)^N/6]\} \\ &\quad \div [1 + (m_c/m_a)\,(1/3 + 2/(N\pi)^2)\sin^2\alpha] \\ &\dot{u}_0 = -v_0\{1 + (m_c/m_a)\,(\sin^2\alpha)[\tfrac{1}{2} - 2/(N\pi)^2 \\ &\quad - 2(-1)^N/(N\pi)^2]\}/[1 + (m_c/m_a)\,(1/3 + 2/(N\pi)^2)\sin^2\alpha]\end{aligned} \tag{19}$$

Nondimensionalization

The first-order approximate nonlinear equations (15-19) have been nondimensionalized to provide the minimum number of independent parameters upon which the dynamic collapse depends. Using the approach of Refs. 13 and 14 with the addition of angle of incidence and periodicity, the following nondimensionalization is introduced:

$$\bar{u}_j = u_j(\cos\alpha)/(\ell\epsilon_E); \quad j = 0,1, \quad \bar{f} = f/r \tag{20}$$

where ϵ_E is the column Euler buckling strain

$$\epsilon_E = (N\pi r/\ell)^2 \tag{21}$$

and the nondimensional time τ

$$\tau = v_0 t(\cos\alpha)/(\ell\epsilon_E)$$

is a measure of the number of Euler displacements $(\ell\epsilon_E)$ which are traversed at the initial velocity v_0. Substitution of Eqs. (20) into Eqs. (15-19) yields

$$\bar{m}\bar{v}^2\bar{u}_0'' + \bar{P} + (-1)^N\bar{\alpha}\bar{v}^2\bar{f}'' = 0 \tag{22}$$

$$\tfrac{1}{2}\bar{v}^2\bar{f}'' + \tfrac{1}{2}(1+\bar{P})\bar{f} + (-1)^N\bar{\alpha}\bar{v}^2\bar{u}_0'' = \bar{e}/2 + \bar{\alpha}\bar{v}^2\bar{u}_1'' \tag{23}$$

with contact condition

$$\bar{u}_1 = \begin{cases} 0, & \text{if } \bar{P}<0 \\ \bar{u}_R, & \text{if } \bar{P}=0 \end{cases} \tag{24}$$

$$\bar{u}_R = \bar{u}_0 + \tfrac{1}{4}(\bar{f}^2 - \bar{e}^2) \tag{25}$$

and initial conditions at $\tau = 0$,

$$\bar{u}_0 = \bar{u}_1 = \bar{u}_1' = 0, \quad \bar{f} = \bar{e}, \quad \bar{f}' = 2\bar{\alpha}, \quad \bar{u}_0' = -1 \tag{26}$$

where $(\,)'$ denotes differentiation with respect to τ. Also, the following nondimensional parameters have been defined:

$$\bar{v} = v_0(\cos\alpha)/[N\pi c(\epsilon_E)^{3/2}]$$

$$\bar{m} = (N\pi)^2 \epsilon_E (m_a/m_c)\cos^2\alpha, \quad \bar{\alpha} = \sqrt{\epsilon_E}(\tan\alpha), \quad \bar{e} = e/r \tag{27}$$

In addition,

$$\bar{P} = P_{\text{avg}}/P_E = \bar{u}_0 - \bar{u}_1 + \tfrac{1}{4}(\bar{f}^2 - \bar{e}^2) \tag{28}$$

where P_E is the static Euler buckling load and c the speed of sound in the column. In deriving Eqs. (22-26) terms of order $\bar{\alpha}^2$ and higher have been neglected. This implies that either α is small (near normal impact) or ϵ_E is small.

The first-order nonlinear equations of motion are coupled through the inertial and nonlinear terms. In general, the response depends only on the four nondimensional parameters given in Eqs. (27) and the number of column bays. These parameters are a velocity parameter $\bar{v}$, a mass parameter $\bar{m}$, an impact angle parameter $\bar{\alpha}$, and an initial imperfection parameter $\bar{e}$. The solution of the initial value problem of Eqs. (22-26) can be studied in terms of these parameters and a comparison of the solution to a more exact analysis is used to determine the range of parametric values in which the first-order approximate nonlinear solution is valid. For $\bar{\alpha}=0$ and $N=1$, the first-order approximate nonlinear equations reduce to Hoff's formulation.[13,14]

Numerical Solution of Equations of Motion

Equations (22-25) in conjunction with the initial conditions of Eqs. (26) may be integrated temporally using the following explicit recursive algorithm,[23]

$$q_{i+1}'' = \tilde{M}^{-1}[F_{i+1} - Q_{i+1} - \tilde{C}q_i' - \tfrac{1}{2}\Delta\tau\tilde{C}q_i'']$$

$$q_{i+1}' = q_i' + \tfrac{1}{2}\Delta\tau(q_i'' + q_{i+1}'')$$

$$q_{i+1} = q_i + \Delta\tau q_i' + \tfrac{1}{2}(\Delta\tau)^2 q_i'' \tag{29}$$

where i refers to the ith time step and $\Delta\tau$ is an appropriate nondimensional time increment. Also,

$$q_i = \begin{Bmatrix} \bar{u}_0 \\ \bar{f} \end{Bmatrix}_i; \quad F_i = \begin{Bmatrix} 0 \\ \bar{e}/2 + \bar{\alpha}\bar{v}^2\bar{u}_{1,i-1}'' \end{Bmatrix}$$

$$Q_i = \begin{Bmatrix} \bar{P}_i \\ \tfrac{1}{2}(1+\bar{P}_i)\bar{f}_i \end{Bmatrix}$$

$$\tilde{M} = \begin{bmatrix} \bar{m}\bar{v}^2 & (-1)^N\bar{\alpha}\bar{v}^2 \\ (-1)^N\bar{\alpha}\bar{v}^2 & \tfrac{1}{2}\bar{v}^2 \end{bmatrix} + \tfrac{1}{2}\tilde{C}\Delta\tau \tag{30}$$

In Eqs. (30), viscous damping has been incorporated through the damping matrix $\tilde{C}$. Furthermore, in solving Eq. (22) the $\bar{u}_1''$ term is treated recursively as a predictor-type term on the right side of the equation. This term vanishes when $\bar{\alpha}$ is zero or when the column is in contact with the surface. Otherwise,

$$\bar{u}_{1,i}'' = \bar{u}_{0,i}'' + \tfrac{1}{2}[(\bar{f}_i')^2 + \bar{f}_i\bar{f}_i'')] \tag{31}$$

Linear Solution

When Eqs. (22) and (23) are linearized, one has

$$\bar{m}\bar{v}^2\bar{u}_0'' + \bar{u}_0 - \bar{u}_1 + (-1)^N\bar{\alpha}\bar{v}^2\bar{f}'' = 0$$

$$\tfrac{1}{2}\bar{v}^2\bar{f}'' + \tfrac{1}{2}\bar{f} + (-1)^N\bar{\alpha}\bar{v}^2\bar{u}_0'' = \bar{e}/2 + \bar{\alpha}\bar{v}^2\bar{u}_1''$$

and the equations are coupled only through the inertial terms. If in addition $\bar{\alpha}=0$, the equations uncouple giving

$$\bar{m}\bar{v}^2\bar{u}_0'' + \bar{u}_0 = \bar{u}_1 \tag{32}$$

$$\bar{v}^2\bar{f}'' + \bar{f} = \bar{e} \tag{33}$$

with

$$\bar{u}_1 = \begin{cases} 0, & \text{if } \bar{P}<0 \\ u_R, & \text{if } \bar{P}=0 \end{cases}$$

and

$$\bar{u}_R = \bar{u}_0 \geq 0$$

As a consequence of the initial conditions of Eqs. (26), $\bar{f}=\bar{e}$ and Eq. (33) reduces to the well-known uniaxial solution

$$\bar{u}_0 = \begin{cases} -\bar{v}\sqrt{\bar{m}}\sin[\tau/(\bar{v}\sqrt{\bar{m}})], & \text{if } \bar{P}<0 \\ \tau - \pi\bar{v}\sqrt{\bar{m}}, & \text{if } \bar{P}=0 \end{cases} \tag{34}$$

Equation (34) may be referred to as the linear dynamic precollapse solution in the same manner that the linear static solution for the straight column is referred to as the linear prebuckling solution. As in the static collapse problem, the deviation of the nonlinear solution from the linear one can be used to help determine the onset of dynamic collapse. The linear solution is displayed in Fig. 2 and constitutes the response when $\bar{e}$ and $\bar{\alpha}$ are zero or the flexural response $\bar{f}$ is small. It is composed of a deformation and restitution phase of equal duration, namely,

$$\tau_d = \tau_R = \pi\bar{v}\sqrt{\bar{m}}/2 \tag{35}$$

The linear solution predicts that the column axial load may exceed the Euler buckling load since $\bar{P}$ may be considerably greater than one. For the linear solution,

$$\bar{P} = \begin{cases} \bar{u}_0 - \bar{u}_1, & \text{if } \bar{u}_0 < 0 \\ 0, & \text{if } \bar{u}_0 \geq 0 \end{cases}$$

In addition, it may be shown that Eqs. (34) and (35) are accurate when $\bar{\alpha}$ is nonzero provided its square is much smaller than $\bar{m}$.

Finite Element Solution

A nonlinear finite analysis has also been performed to study the column impact problem. Results were generated using a computer code whose development followed Belytschko's convected transient analysis procedure.[23,24] Because of the nature of the procedure, no artificial strains are introduced due to rigid-body rotation of an element. Consequently, the procedure can allow unlimited rotations.

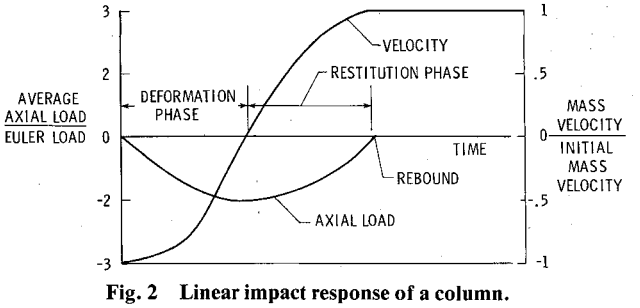

Fig. 2 Linear impact response of a column.

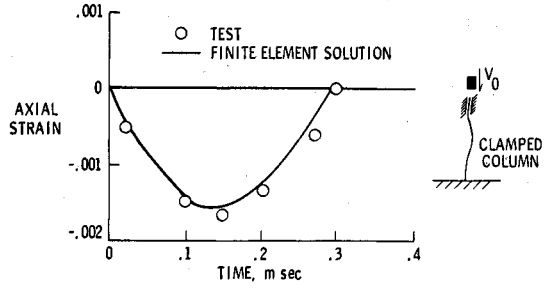

Fig. 3 Comparison of test and analysis for axial impact of a mass on a clamped column.

Belytschko has validated the procedure on many benchmark cases.[23,24] Those cases which involved impact response were used to validate the computer code developed for this study. In addition, the results of the code compare very well with the experimental response of a clamped column axially loaded at one end by an impinging mass.[22] Comparison between the finite element results and test data for the column midpoint axial strain is shown in Fig. 3 for the time duration in which the mass and column are in contact. With the exception of the clamped boundary conditions, the experiment and the present problem are very similar during the time the mass and column end are in contact and this is reflected in the good agreement shown.

Coefficient of Restitution

As already mentioned, the linear solution consists of one cycle of motion composed of a deformation and restitution phase of equal duration. However, for the nonlinear solution, this will not generally be true. Instead, the impact response will consist of many cycles of motion, each composed of a deformation phase followed by a restitution phase of unequal duration. Several such cycles may occur while the end of the column is in contact or near the rigid surface so that a sequence of several impacts and rebounds is possible. However, the first cycle is usually of primary significance to the nature of the response. Since the column is assumed to be purely elastic with no external energy dissipation mechanisms, the column must eventually leave the surface permanently and thus a complete or permanent collapse is not possible. However, insight into the complete collapse is gained from the elastic response by examining the coefficient of restitution C_R.

For the purpose of this paper the primary coefficient of restitution is expressed as the ratio of the velocity of the attached mass when the end of the column loses contact with the rigid surface to the initial impact velocity of the attached mass. Thus, for the first cycle

$$C_R = (\dot{u}_0)_{\bar{P}_1=0}/v_0 = (\bar{u}_0')_{\bar{P}_1=0} \tag{36}$$

where $\bar{P}_1$ is the ratio of the column axial load at the surface ($x=0$) to the Euler load. That is,

$$\bar{P}_1 = \bar{u}_0 - \bar{u}_1 + \tfrac{1}{2}(\bar{f}^2 - \bar{e}^2)$$

It is recognized that the definition of C_R used herein is not the usual definition where the velocity at the end of the restitution phase is used rather than the velocity when contact is lost. The two values are not necessarily the same.

The coefficient of restitution takes on values between zero and one. When C_R is unity or zero, the impact is often designated "elastic" or "plastic," respectively. The designations are somewhat misleading since C_R can go to zero even for the completely elastic system. Nevertheless, the designations rightfully indicate that as C_R goes to zero the column approaches a collapse condition which would probably occur were plasticity present. In addition, the coefficient provides insight into the column's deformation mode. This may be seen by a consideration of the energies involved in the response.

Energy Considerations

At the time of initial impact, the total energy is all kinetic energy T_I. After impact, some of this kinetic energy may remain with the mass T_m or some may go into extensional strain energy (or axial wave energy which is neglected here), flexural strain energy U_f, or flexural kinetic energy T_f. In particular at rebound, the extensional stored energy is zero inasmuch as $\bar{P}$ is zero. Thus one has

$$T_m + T_f + U_f = T_I \tag{37}$$

Depending on the values of the governing parameters [Eqs. (27)], the column may rebound and leave the surface without its deformation going beyond the linear precollapse state. Such a case is shown in Fig. 2 where the rebound velocity of the attached mass equals the initial impact velocity, both the kinetic and strain energies due to flexure vanish at rebound, and the primary coefficient of restitution C_R has a value of one. However, if the parameters are such that the column stays in contact with the rigid surface past the linear precollapse state, then at rebound the maximum energy in flexural deformation and motion occurs when the kinetic energy of the attached mass vanishes. For this case, C_R also vanishes, implying that all of the energy of impact has gone into column flexure. If the structure had sufficient plasticity, the flexural energy would be dissipated in plastic work and no energy would be available for rebound. Thus, values of the

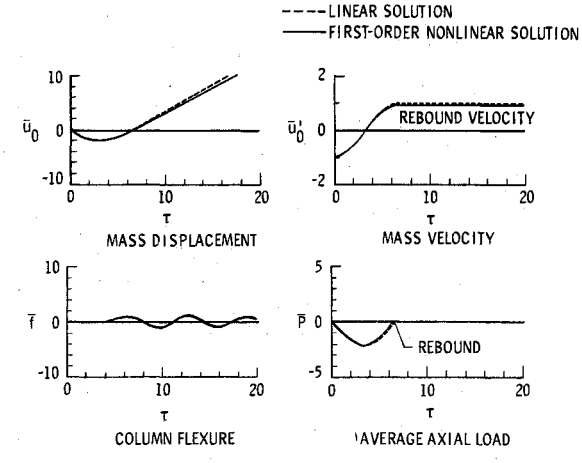

Fig. 4 Column response in the transition region where $\bar{m}=4.5$, $\bar{v}=1.0$, $\bar{e}=0.01$, and $\bar{\alpha}=0.0$.

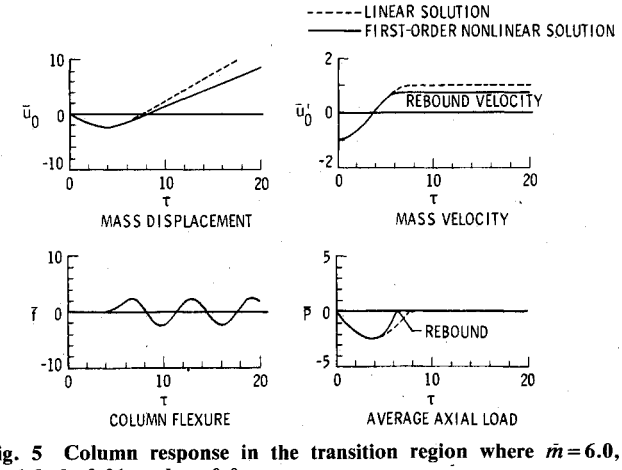

Fig. 5 Column response in the transition region where $\bar{m}=6.0$, $\bar{v}=1.0$, $\bar{e}=0.01$, and $\bar{\alpha}=0.0$.

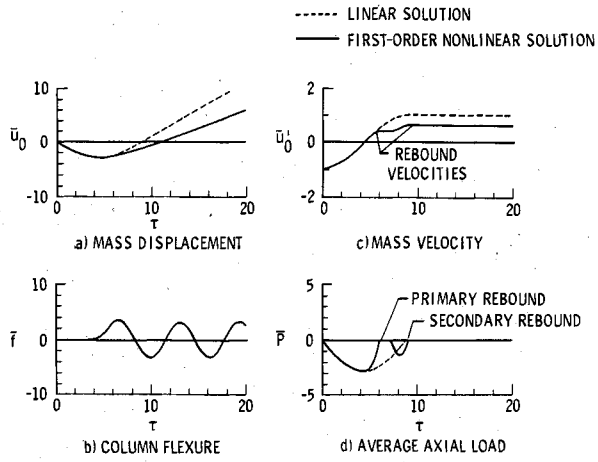

Fig. 6 Column response in the transition region where $\bar{m}=8.0$, $\bar{v}=1.0$, $\bar{e}=0.01$, and $\bar{\alpha}=0.0$.

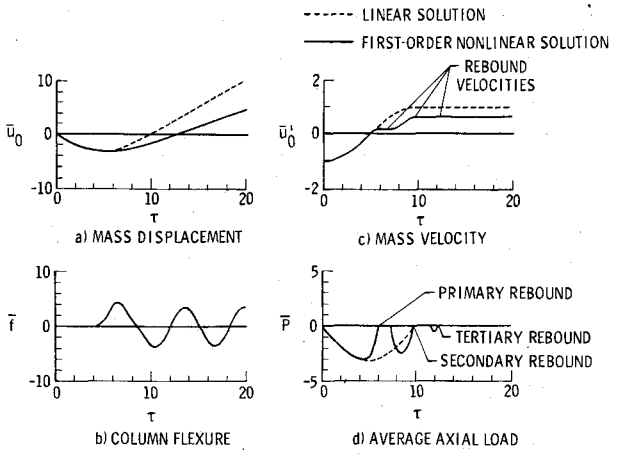

Fig. 7 Column response in the transition region where $\bar{m}=10.1$, $\bar{v}=1.0$, $\bar{e}=0.01$, and $\bar{\alpha}=0.0$.

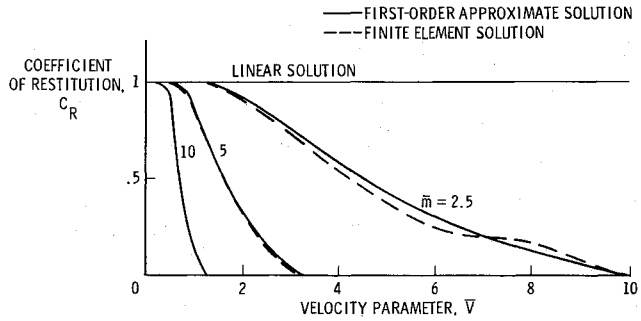

Fig. 8 Sensitivity of the primary coefficient of restitution to the mass parameter when $\bar{\alpha}=0.0$ and $\bar{e}=0.01$.

governing parameters which make C_R vanish are of prime importance to the collapse.

Discussion of Results

General Remarks

Numerical results are presented to indicate the effect of the nondimensional parameters on the impact response of an elastic periodically supported column. Parametric studies were performed for single-bay columns since, for a zero value of the impact angle parameter, the governing nondimensional equations (22-26) are independent of the number of periodic bays.

The effect of initial imperfections is well documented by Hoff[13,14] for a similar problem wherein $\bar{\alpha}=0$ and $\bar{m}$ is infinite; thus, the scope of this paper is limited to a small initial imperfection $\bar{e}$ (either 0 or 0.01).

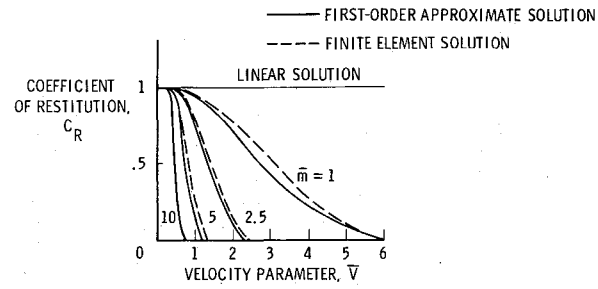

Fig. 9 Sensitivity of the primary coefficient of restitution to the mass parameter when $\bar{\alpha}=0.05$ and $\bar{e}=0.01$.

Effect of Mass and Impact Velocity Parameters

The transient response of a column for various values of $\bar{m}$ and a fixed set of $\bar{v}$, $\bar{\alpha}$, and $\bar{e}$ is illustrated in Figs. 4-7. Each figure depicts the variation with τ of the displacement and velocity of the attached mass, the flexural displacement of the column, and the average axial load of the column. The solid curves are derived from the first-order approximate nonlinear solution [Eqs. (22-26)], while the dashed curves are derived from the linear solution [Eqs. (32-34)].

Each of Figs. 4-7 and others similar to these may be used to determine a value of the primary coefficient of restitution C_R as defined in Eq. (36). When this is accomplished for various values of $\bar{m}$ and $\bar{v}$, curves such as those shown in Figs. 8 ($\bar{\alpha}=0$) and 9 ($\bar{\alpha}=0.05$) result. As discussed previously, the value of C_R is a measure of the deviation of the nonlinear solution from the linear solution. For a value of C_R near one, the nonlinear effects due to flexure are negligible. As the value of C_R decreases to zero, the nonlinear effects become increasingly more dominant until C_R vanishes and all motion of the column becomes flexural motion. As such, two critical values of C_R are defined as follows: a value near the linearly predicted value of one (say, 0.98) and another when C_R vanishes. Figures 8 and 9 indicate the existence of these two critical values of C_R. Curves representing combinations of $\bar{m}$ and $\bar{v}$ which bring about these critical conditions are collected and displayed as interaction curves in Figs. 10 and 11. These interaction curves are not lines of constant momentum since they do not plot as straight lines with slope of negative one on log-log scales.

The interaction curves define three regions of the nondimensional parameters in which the response takes on distinctive characteristics. These regions are designated as linear, transition, and dynamic collapse. The reasoning behind the choice of these names becomes evident with further discussion. The interaction curve separating the linear and transition regions is shown hatched inasmuch as the condition of $C_R=0.98$ which defines the curve was arbitrarily chosen. In any case, C_R is within 2% of unity in the linear region, varies between 0.98 and 0 in the transition region, and vanishes in the collapse region.

Also shown in each of Figs. 10 and 11 is a dashed line derived from the linear dynamic solution. For values of $\bar{m}$ and $\bar{v}$ lying on the line, the peak axial compressive load equals the static Euler buckling load. Thus, for values of $\bar{v}$ and $\bar{m}$ lying below or above this line, the peak axial compressive load will be less than or greater than the Euler load, respectively.

The interaction curves of Figs. 10 and 11 indicate that as $\bar{m}$ goes to infinity and $\bar{v}$ goes to zero, the static buckling condition is approached. This situation is similar to a column in a displacement-controlled testing machine where the loading head moves at a constant slow velocity.[13,14] In addition, as the static buckling condition is approached, the interaction curves approach the dashed line which represents the static Euler buckling condition and the transition region shrinks to zero.

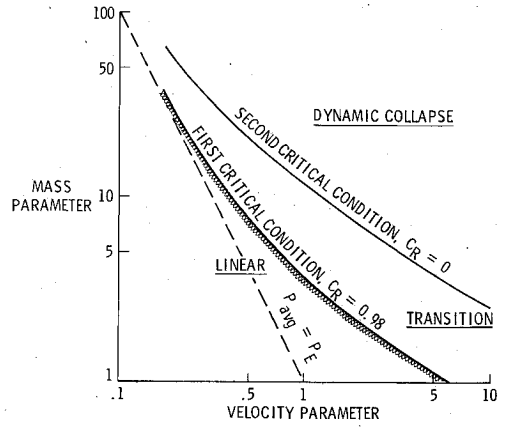

Fig. 10 Interaction curves and response regions for a column with an initial imperfection ($\bar{e} = 0.01$) under a normal impact ($\bar{\alpha} = 0.0$).

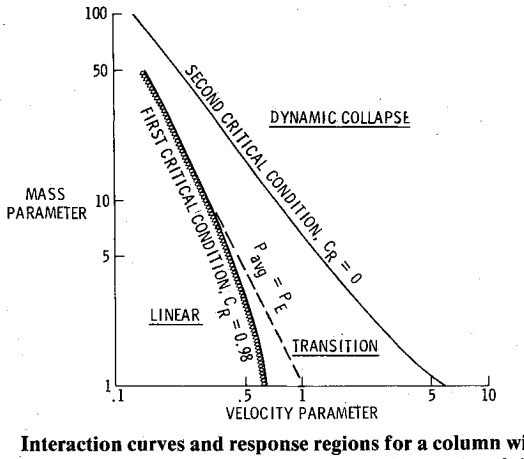

Fig. 11 Interaction curves and response regions for a column with an initial imperfection ($\bar{e} = 0.01$) under a non-normal impact ($\bar{\alpha} = 0.05$).

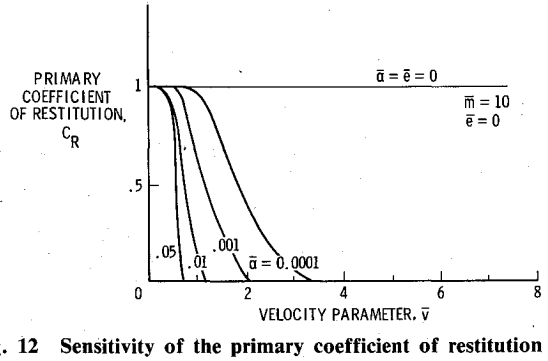

Fig. 12 Sensitivity of the primary coefficient of restitution to the impact angle parameter when $\bar{m} = 10.0$ and $\bar{e} = 0.0$.

Effect of Impact Angle Parameter

The impact angle parameter $\bar{\alpha}$ plays a significant role in determining the column response by initiating column flexure in much the same manner as the initial imperfection parameter $\bar{e}$ does for the case of a normal impact. When both $\bar{e}$ and $\bar{\alpha}$ are zero, only the linear solution (i.e., $C_R = 1$) is possible. Thus, to achieve flexure in the response, either $\bar{\alpha}$ or $\bar{e}$ must be nonzero. When $\bar{\alpha} = 0$, the response has been shown[13] to be sensitive to $\bar{e}$ and Fig. 12 indicates that the response is also very sensitive to $\bar{\alpha}$ even for very small values of $\bar{\alpha}$.

Variation of C_R with $\bar{v}$ up to the collapse region for values of $\bar{\alpha}$ ranging from 0 to 0.05 is shown in Fig. 12 for a fixed set of $\bar{m}$ and $\bar{e}$ (e.g., the value of $\bar{\alpha}$ equal to 0.05 can correspond to a column with Euler buckling strain of 0.005 and an impact angle of approximately 35 deg from the normal). As $\bar{\alpha}$ increases, the impact response becomes less sensitive to $\bar{\alpha}$ for a given value of $\bar{v}$. However, this does not mean that the impact response becomes less sensitive to the impact angle α as $\bar{\alpha}$ increases since the definition of $\bar{v}$ depends on $\cos\alpha$ and $\bar{\alpha}$ depends on $\tan\alpha$. Rather, it means, for example, that if the solution for $\bar{\alpha} = 0.05$ is known, the solution for values of $\bar{\alpha}$ greater than 0.05 can be approximated by simply using the nondimensional parameter definitions of Eqs. (27).

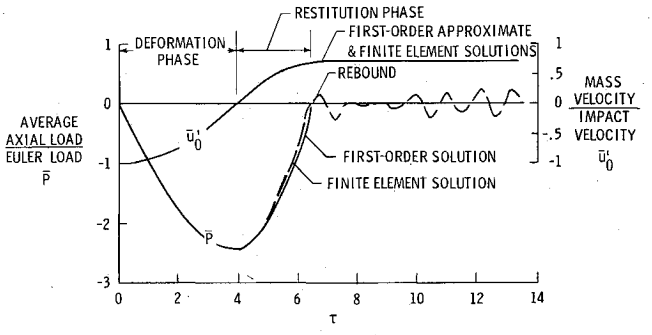

Fig. 13 Comparison of typical first-order approximate and finite element nonlinear responses in the transition region ($\bar{m} = 6.0$, $\bar{v} = 1.0$, $\bar{e} = 0.01$, and $\bar{\alpha} = 0.0$).

A comparison of Fig. 12 for the case of $\bar{\alpha} = 0.05$, $\bar{e} = 0$, and $\bar{m} = 10$ with Fig. 9 for the case of $\bar{\alpha} = 0.05$, $\bar{e} = 0.01$, and $\bar{m} = 10$ indicates that $\bar{e}$ has little effect on the response when $\bar{\alpha} = 0.05$. Thus, as the impact angle parameter is increased, the effect of the initial imperfection parameter becomes relatively unimportant. Furthermore, in the presence of a nonzero $\bar{\alpha}$, the size of the linear region is reduced for low values of $\bar{m}$, i.e., axial-flexural coupling occurs at lower values of $\bar{v}$ and $\bar{m}$ as $\bar{\alpha}$ increases.

Linear and Transition Regions

Attributes

The values of the nondimensional parameters used for the normal impact transient responses shown in Figs. 4-7 correspond to the transition region of Fig. 10. The response in the transition region deviates significantly from the linear solution in certain respects. Comparison with the linear solution indicates that for the parameter values shown in Figs. 4-7, the duration of the restitution phase prior to the primary rebound and the rebound velocity are reduced from that predicted by the linear solution. Conversely, the duration of the deformation phase is nearly equal to that predicted by the linear solution.

The most important attribute of the linear and transition regions is that, for parameters lying in these regions, both the linear and nonlinear solutions predict the same peak axial compressive load. The peak load exceeds the static Euler buckling load P_E for values of $\bar{v}$ and $\bar{m}$ lying above the dashed line of Fig. 10 on which P equals P_E. For normal impacts, Fig. 10 shows that this line lies entirely in the linear region. Therefore, peak axial compressive loads in the transition and collapse regions will be greater than P_E.

Previous researchers[18,22] have emphasized that the dynamic load may exceed the static by referring to this situation as a "supercritical" condition or a "dynamic load factor." However, this is purely a linear dynamic effect and is unrelated to collapse or nonlinear response.

Though not shown, transient responses for non-normal impact ($\bar{\alpha}$ nonzero) indicate similar attributes for the linear and transition regions. However, the static Euler buckling line may lie in the transition region as shown in Fig. 11. Thus the peak axial compressive load may be less than the Euler load in the transition region.

As discussed earlier, the column response may consist of one or more rebounds. The first rebound is referred to as the "primary" rebound. In Figs. 4 and 5, the column separates

from the surface permanently after one rebound, while in Figs. 6 and 7 two and three rebounds, respectively, occur before permanent separation. Each rebound is associated with a velocity plateau in the c portion of each figure and the termination of an axial compression half-wave in the d portion. Considerable flexural vibration is excited by the impact and continues after separation. The flexural energy accounts for most of the difference between the initial impact and final rebound kinetic energies.

Validity of First-Order Approximate Nonlinear Solution

For comparison, Figs. 8 and 9 contain predictions of C_R based upon the first-order approximate and finite element solutions. Agreement is very good; however, the first-order approximate solution may lose its validity when predicting C_R at high values of $\bar{v}$ or $\bar{m}$. In general, the first-order approximate solution is valid in the linear and transition regions provided neither $\bar{v}$ nor $\bar{m}$ are very large.

In Fig. 13, the first-order approximate and finite element nonlinear responses are compared in the transition region. Agreement is excellent with the exception of the axial wave motion which dominates the $\bar{P}$ response after rebound for the finite element solution. The effects of axial inertia were included in the finite element solution but neglected in the first-order approximate solution.

Collapse Region

Attributes

The most important characteristic of the collapse region is the reduction of the peak axial compressive load from the linearly predicted value. Thus, the situation is analogous to the static case wherein the linearly predicted infinite load is never reached due to the presence of geometric nonlinearities which give rise to buckling. The peak load is directly related to the deceleration of the mass [via Eq. (22)] and is therefore of primary importance to the impact problem.

In Fig. 14, the variation with $\bar{m}$ of the nondimensional average peak axial compressive load prior to rebound is shown for different values of $\bar{v}$. Solid lines denote the response in the linear region, dotted lines denote the transition region, and dashed lines denote the collapse region. Predictions based upon the linear solutions, first-order approximate nonlinear solutions, and finite element nonlinear solutions are given. For low values of $\bar{v}$, the nonlinear solutions are in excellent agreement with each other, but for high values of $\bar{v}$ they tend to deviate. For $\bar{v}=10$, the first-order approximate solution is as much as 15% higher than the finite element prediction. This difference is attributed to axial inertia effects which are neglected in the first-order approximate solution. Nevertheless, both nonlinear solutions predict a reduction in the peak axial compressive load from the linear peak value. As $\bar{m}$ increases, the nonlinear solutions approach ultimate load values, whereas the linear dynamic solution continues to grow without bound. Since the peak value of $\bar{P}$ is greater than one, the ultimate dynamic collapse load is greater than the static Euler buckling load. No substantial reduction from the linearly predicted peak load occurs unless $\bar{m}$ and $\bar{v}$ lie in the collapse region.

The criterion often used in statics problems for the collapse of columns is buckling. At buckling, the column carries its maximum load and deviates from the infinite static linear solution. Extending this observation to the dynamic case, Fig. 14 indicates that the deviation of the peak axial compressive load from that of the linear solution occurs approximately when the collapse region is entered (i.e., $\bar{m}$ and $\bar{v}$ are such that C_R is zero). Then a reduction from the linearly predicted peak load occurs. Of course, in the dynamic case the solution is not only a function of the column geometry, but in addition depends upon the mass and velocity parameters. As a consequence, when the collapse region is just entered, the reduction from the linear to the nonlinear solution is a

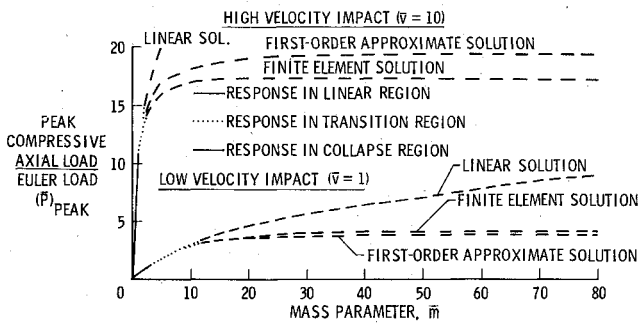

Fig. 14 Variation of the peak axial compressive load with the mass parameter for high and low impact velocities when $\bar{e}=0.01$ and $\bar{\alpha}=0.0$.

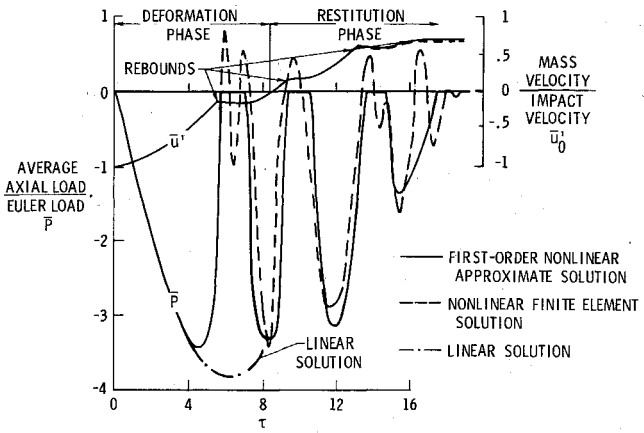

Fig. 15 Comparison of typical first-order approximate and finite element nonlinear responses in the collapse regon ($\bar{m}=14.0$, $\bar{v}=1.0$, $\bar{e}=0.01$, and $\bar{\alpha}=0.0$).

gradual process and not as dramatic as in the static case. This reduction or nonlinear knockdown from the linear dynamic value increases with increasing values of $\bar{m}$ and $\bar{v}$. Thus in designing columns for axial impact, the nonlinear knockdown from the linear dynamic peak load should be considered rather than the load factor for magnifying the static Euler buckling load. The designation of the third region as "collapse" is thereby a reasonable extension of the static buckling criterion. This dynamic collapse criterion based on C_R vanishing is similar to one used previously[22] where an abrupt change in the peak axial strain with increasing velocity was employed.

Validity of First-Order Approximate Nonlinear Solution

In Fig. 15, the first-order approximate and finite element nonlinear responses are compared in the collapse region. Both analyses predict the duration of the deformation phase to be about 8.3, which is considerably longer than the linearly predicted value from Eq. (35) of 6.1. In addition, both analyses reveal a sequence of small rebounds. These are characterized by the plateaus in the $\bar{u}'_0$ curve and by the associated vanishing of $\bar{P}$ for the first-order approximate solution or the relatively small oscillations of $\bar{P}$ about zero for the finite element solution. Since the values of $\bar{m}$ and $\bar{v}$ lie in the collapse region, the primary coefficient of restitution associated with the first plateau in $\bar{u}'_0$ is negative and has no physical meaning inasmuch as the mass is still moving toward the surface.

Because the system is elastic, the column eventually leaves the surface permanently, but the duration of contact with the surface is about 18.0, while the linear value from Eq. (35) is 12.2. As the values of $\bar{m}$ and $\bar{v}$ lie further into the collapse region, the deformation and restitution phases will continue

to increase. Consequently, it is anticipated that for parametric values lying in this region, the column will suffer a complete collapse if plasticity is included.

Conclusions

An analytical investigation of the dynamic collapse of an elastic periodically supported column having an attached mass at one end and impacting a rigid surface with prescribed velocity and angle of incidence at the other end has been performed. The investigation has been carried out using a first-order approximate nonlinear solution and a nonlinear finite element solution. The first-order approximate nonlinear solution has led to the determination of four basic non-dimensional parameters which govern the response. These parameters include mass, impact velocity, initial imperfection, and impact angle parameters. Three regions of these parameters have been identified in which the response character is vastly different. These regions have been designated as linear, transition, and collapse. Threshold values of the parameters which separate these regions have been defined.

For parameters lying in the linear region, the response is dominated by axial motion and the rebound velocity is equal to the impact velocity. In the transition region, some axial-flexural coupling occurs which results in a reduction of the rebound velocity from the linearly predicted value. However, the duration of the deformation phase of the impact response as well as the peak axial compressive load are nearly the same as those predicted by the linear dynamic solution. For normal impact, the peak axial compressive load exceeds the static Euler buckling load for parameters lying in the transition or collapse regions. For non-normal impact, axial-flexural coupling occurs for parameters lying in the transition region, but the peak axial compressive load may be less than the static Euler buckling load.

For parameters lying the collapse region, the response is flexure dominated. As a consequence, the rebound velocity is reduced from that of the linear region, and the duration of the deformation phase becomes considerably longer than that of the other two regions. Most importantly, in the collapse region, the peak axial compressive load carried by the column is reduced considerably from that predicted by the linear dynamic solution, but exceeds the static Euler buckling solution. As the mass parameter is increased in the collapse region, the peak axial compressive load quickly approaches an ultimate dynamic value whereas the linear solution predicts an unbounded compressive load.

Comparison of the first-order approximate nonlinear solution and the finite element nonlinear solution indicates that, provided the values of mass and velocity parameters are not too high, the first-order approximate solution provides excellent results in the linear and transition regions and very good results in the collapse region.

Acknowledgment

The authors would like to thank Louis Gutierrez, a Co-op student from the University of Puerto Rico for his valuable help in generating a large portion of the numerical results from the finite element computer code.

References

[1] Thomson, R. G. and Goetz, R. C., "NASA/FAA General Aviation Crash Dynamics Program—A Status Report," AIAA Paper 79-0780, April 1979.

[2] Pifko, A. B., Levine, H. S., and Armen, H. Jr., "PLANS—A Finite Element Program for Nonlinear Analysis of Structures; Vol. 1—Theoretical Manual," NASA CR-2568, Nov. 1975.

[3] Wittlin, G., "Development, Experimental Verification and Application of Program KRASH for General Aviation Airplane Structural Crash Dynamics," FAA-RD-78-119, Dec. 1978.

[4] Kamat, M. P., "Survey of Computer Programs for Prediction of Crash Response and of Its Experimental Validation," *Measurement and Prediction of Structural and Biodynamic Crash-Impact Response*, ASME, New York, 1976, pp. 33-48.

[5] Pifko, A. B. and Winter, R., "Theory and Application of Finite Element Analysis to Structural Crash Simulation," *Computers and Structures*, Vol. 13, June 1981, pp. 277-285.

[6] Wittlin, G., Bloedel, A. W., and Ahrens, D. J., "Experimental Verification of Program KRASH—Mathematical Model for General Aviation Structural Crash Dynamics," Paper 790589 presented at SAE Business Aircraft Meeting and Exposition, April 1976.

[7] Winter, R., Pifko, A. B., and Cronkhite, J. D., "Crash Simulation of Composite and Aluminum Helicopter Fuselages Using a Finite Element Program," Paper 79-0781 presented at AIAA/ASME/ASCE/AHS 20th Structures, Structural Dynamics, and Materials Conference, April 1979.

[8] Winter, R., Pifko, A. B., and Armen, H. Jr., "Crash Simulations of Skin Frame Structures Using a Finite Element Code," Paper 770484 presented at SAE Business Aircraft Meeting and Exposition, March-April 1977.

[9] Wittlin, G., "Summary of Results for a Twin-Engine, Low-Wing Airplane Substructure Crash Impact Condition Analyzed with Program KRASH," FAA-RD-79-13, Feb. 1979.

[10] Hayduk, R. J., Thomson, R. G., Wittlin, G., and Kamat, M. P., "Nonlinear Structural Crash Dynamics Analysis," Paper 790588 presented as SAE Business Aircraft Meeting and Exposition, April 1979.

[11] Wittlin, G. and Gamon, M. A., "Experimental Program for the Development of Improved Helicopter Structural Crashworthiness Analytical and Design Techniques," USAAMRDL TR 72-72, May 1973.

[12] Castle, C. B. and Alfaro-Bou, E., "Light Airplane Crash Test at Three Flight Path Angles," NASA TP-1210, June 1978.

[13] Hoff, N. J., Nardo, S. V., and Erickson, B., "The Maximum Load Support by an Elastic Column in a Rapid Compression Test," *Proceedings of the 1st U.S. National Congress of Applied Mechanics*, AMSE, Chicago, June 1951, pp. 419-423.

[14] Hoff, N. J., "The Dynamics of the Buckling of Elastic Columns," *Journal of Applied Mechanics, Transactions of ASME*, Vol. 18, March 1951, pp. 68-74.

[15] Davidson, J. F., "Buckling of Struts Under Dynamic Loading," *Journal of Mechanics and Physics of Solids*, Vol. 2, Oct. 1953, pp. 54-66.

[16] Gerard, G. and Becker, H., "Column Behavior Under Conditions of Impact," *Journal of Aeronautical Sciences*, Vol. 19, Jan. 1952, pp. 58-60.

[17] Sevin, E., "On the Elastic Bending of Columns Due to Dynamic Axial Forces Including Effects of Axial Inertia," *Journal of Applied Mechanics, Transactions of ASME*, Vol. 27, No. 1, March 1960, pp. 125-131.

[18] Housner, G. W. and Tso, W. K., "Dynamic Behavior of Supercritically Loaded Struts," *Journal of the Engineering Mechanics Division, Proceedings of ASCE*, Vol. 88, No. EM5, Oct. 1962, pp. 41-65.

[19] Hayashi, T. and Sano, Y., "Dynamic Buckling of Elastic Bars, 1st Report, The Case of Low Velocity Impact," *Bulletin of the JSME*, Vol. 15, No. 88, 1972, pp. 1167-1175.

[20] Hayashi, T. and Sano, Y., "Dynamic Buckling of Elastic Bars, 2nd Report, The Case of High Velocity Impact," *Bulletin of the JSME*, Vol. 15, No. 88, 1972, pp. 1176-1184.

[21] McIvor, I. K. and Bernard, J. E., "The Dynamic Response of Columns Under Short Duration Axial Loads," *Journal of Applied Mechanics, Transactions of ASME*, Vol. 40, No. 3, Sept. 1973, pp. 688-692.

[22] Ari Gur, J., Weller, T., and Singer, J., "Theoretical Studies of Columns Under Axial Impact and Experimental Verification," Technion—Israel Institute of Technology, TAE No. 377, Aug. 1979.

[23] Belytschko, T. and Hsieh, B. J., "Nonlinear Transient Finite Element Analysis with Convected Coordinates," *International Journal for Numerical Methods in Engineering*, Vol. 7, 1973, pp. 255-272.

[24] Belytschko, T., Welch, R. E., and Bruce, R. W., "Large Displacement Nonlinear Transient Analysis by Finite Elements," *Proceedings of International Conference on Vehicle Structural Mechanics*, SAE, Warrendale, Pa., 1974, pp. 188-197.